Revista Mexicana de Astronomía y Astrofísica Revista mexicana de astronomía y astrofísica ISSN: 0185-1101 Instituto de Astronomía, UNAM

Tejeda, Emilio
Incompressible wind accretion
Revista mexicana de astronomía y astrofísica, vol. 54, no. 1, 2018, pp. 01-08
Instituto de Astronomía, UNAM

DOI: https://doi.org/10.14482/INDES.30.1.303.661

Available in: https://www.redalyc.org/articulo.oa?id=57171626012



Complete issue

More information about this article

Journal's webpage in redalyc.org



Scientific Information System Redalyc

Network of Scientific Journals from Latin America and the Caribbean, Spain and Portugal

Project academic non-profit, developed under the open access initiative

# INCOMPRESSIBLE WIND ACCRETION

Emilio Tejeda

Instituto de Astronomía, UNAM, México

Received November 21 2017; accepted January 4 2018

## ABSTRACT

We present a simple, analytic model of an incompressible fluid accreting onto a moving gravitating object. This solution allows us to probe the highly subsonic regime of wind accretion. Moreover, it corresponds to the Newtonian limit of a previously known relativistic model of a stiff fluid accreting onto a black hole. Besides filling this blank in the literature, the new solution should be useful as a benchmark test for numerical hydrodynamics codes. Given its simplicity, it can also be used as an illustrative example in a gas dynamics course.

## RESUMEN

Presentamos un modelo analítico sencillo de un fluido incompresible que acrece hacia un objeto gravitacional en movimiento. Esta solución nos permite estudiar el régimen altamente subsónico de acreción de viento. Adicionalmente, esta solución corresponde al límite newtoniano de un modelo relativista ya conocido de un fluido con ecuación de estado rígida que acrece hacia un agujero negro. Además de llenar este espacio en blanco en la literatura, el nuevo modelo podrá ser de utilidad como una prueba de referencia para códigos numéricos de hidrodinámica. Dada su simplicidad, también se puede usar como un ejemplo ilustrativo como parte de un curso de dinámica de fluidos.

Key Words: hydrodynamics — methods: analytical — stars: winds, outflows

## 1. INTRODUCTION

The study of wind accretion phenomena has been an active field of research since the pioneering work of Hoyle & Lyttleton (1939) and Bondi & Hoyle (1944). In its basic formulation, this problem deals with the accretion flow onto a massive, gravitating object traveling at a constant velocity across an otherwise unperturbed, homogeneous gaseous medium. Alternatively, this same situation can be reversed to consider instead a constant wind accreting onto a massive object held fixed at the origin of coordinates. The Bondi-Hoyle-Lyttleton model (BHL hereafter) provides an analytic description of this problem by approximating the incoming accretion flow by ballistic trajectories. Other analytic solutions have been found in the spherically symmetric case (zero relative velocity between the accretor and the ambient gas, Bondi 1952; Michel 1972) as well as for the relativistic wind accretion of a stiff fluid (Petrich, Shapiro, & Teukolsky 1988, PST hereafter). Further advances have been mostly based on numerical studies, both in the Newtonian (Hunt 1971; Ruffert & Arnett 1994; Shima et al. 1985) and relativistic regimes (Petrich et al. 1989; Font & Ibáñez 1998; Zanotti et al. 2011), as well as on the stability of the resulting accretion flow (Matsuda et al. 1991; Foglizzo et al. 2005; Cruz-Osorio et al. 2012). For a general review on wind accretion see Edgar (2004).

In this article we present an analytic solution for an incompressible fluid accreting onto a moving massive object. The solution is based on the assumptions of stationarity, axisymmetry and irrotational flow. The accretor, which we shall treat as a perfect sink of gas, interacts with the fluid via a Newtonian gravitational potential, while the self-gravity of the fluid is neglected.

The relativistic solution found by PST describes a stiff fluid accreting onto a moving black hole. With the stiff equation of state adopted by PST, the fluid's sound speed equals the speed of light everywhere. Because of this, the PST model was thought to have no Newtonian analogue. With this article, however, we intend to fill a blank in the literature by showing

that the incompressible flow presented here corresponds to the non-relativistic limit of the PST solution.

It is customary to characterize a given wind flow in terms of the asymptotic Mach number  $\mathcal{M} = v_{\infty}/a_{\infty}$ , where  $v_{\infty}$  is the wind velocity and  $a_{\infty}$ the speed of sound, both measured far away from the central accretor. In terms of this parameter, the BHL model is well suited to study a supersonic regime with  $\mathcal{M} \gg 1$ , where the ballistic treatment is a valid approximation given that the fluid cannot oppose pressure gradients readily (effectively behaving as infinitely compressible). At the other end of the spectrum, the incompressible approximation is valid in the subsonic regime with  $\mathcal{M} \simeq 0$  (the sound speed in an incompressible fluid can be considered as infinitely large). We expect then to contribute to a better understanding of accretion phenomena by studying this extreme regime.

Although usually based on highly idealized assumptions, analytic solutions are useful to guide our intuition and to understand the basic principles behind a physical problem. Moreover, analytic solutions are valuable as benchmark tools for developing and testing numerical codes. Indeed, both the BHL and PST models have been successfully used to this end in several numerical studies (Banyuls et al. 1997; Duez et al. 2008; Moeckel & Throop 2009). Then, in spite of the incompressible flow approximation having a rather limited applicability in astrophysics, we propose that the analytic model presented in this article also can be useful as a benchmark solution.

## 2. ANALYTIC SOLUTION

Consider a steady wind passing by a gravitating object of mass M that sits at the origin of coordinates. We assume that the gas consists of an incompressible fluid described by a constant density  $\rho_{\infty}$  and two variables: its pressure P and a velocity field  $\vec{v}$ . Furthermore, we take the central object as a spherically symmetric, perfect sink of gas. Far away from the central object, the fluid is described by the asymptotic boundary conditions

$$P|_{\infty} = P_{\infty},\tag{1}$$

$$\vec{v}|_{\infty} = v_{\infty} \,\hat{z},\tag{2}$$

where we have aligned the z axis with the incoming wind direction.

In general, for a single perfect fluid the flow dynamics will be governed by the continuity and Euler equations:

$$\frac{\partial \rho}{\partial t} + \nabla \cdot (\rho \, \vec{v}) = 0, \tag{3}$$

$$\frac{\partial \vec{v}}{\partial t} + \vec{v} \cdot \nabla \vec{v} = -\frac{1}{\rho} \nabla P - \frac{GM}{r^2} \hat{r}.$$
 (4)

Under the assumptions of stationarity and incompressibility, equation (3) reduces to

$$\nabla \cdot \vec{v} = 0, \tag{5}$$

while integration of equation (4) leads to the Bernoulli constant

$$B = \frac{v^2}{2} + \frac{P}{\rho_{\infty}} - \frac{GM}{r} = \frac{v_{\infty}^2}{2} + \frac{P_{\infty}}{\rho_{\infty}},\tag{6}$$

where we have imposed the boundary conditions in equations (1) and (2).

The boundary condition for the velocity field at infinity in equation (2) corresponds to an irrotational flow, i.e.  $\nabla \times \vec{v} = 0$ . Given the axisymmetry of the problem and assuming a smooth laminar flow, we shall expect this condition to hold everywhere else. We can then propose a velocity potential  $\Phi$  such that  $\vec{v} = \nabla \Phi$  which, according to equation (5), satisfies the Laplace equation

$$\nabla^2 \Phi = 0. \tag{7}$$

Adopting spherical coordinates, we can write the well known solution to this equation as (Jackson 1998)

$$\Phi = \sum_{n=0}^{\infty} \left( A_n \, r^n + B_n \, r^{-(n+1)} \right) P_n(\cos \theta), \tag{8}$$

where  $A_n$  and  $B_n$  are constant coefficients and  $P_n(\cos \theta)$  is the Legendre polynomial of degree n. With these same coordinates, the boundary condition in equation (2) is

$$|\vec{v}|_{\infty} = v_{\infty} \,\hat{z} = v_{\infty} \left(\cos\theta \,\hat{r} - \sin\theta \,\hat{\theta}\right),$$
 (9)

from where it follows that

$$\left. \left( \frac{\partial \Phi}{\partial r} \right) \right|_{\infty} = \left. \left( \frac{\mathrm{d}r}{\mathrm{d}t} \right) \right|_{\infty} = v_{\infty} \, \cos \theta, \qquad (10)$$

$$\left. \left( \frac{1}{r} \frac{\partial \Phi}{\partial \theta} \right) \right|_{\infty} = \left. \left( r \frac{\mathrm{d}\theta}{\mathrm{d}t} \right) \right|_{\infty} = -v_{\infty} \sin \theta. \tag{11}$$

 $<sup>^1 {\</sup>rm The}$  classic Bondi (1952) solution for spherical accretion corresponds as well to the subsonic limit with  $\mathcal{M}=v_\infty/a_\infty\simeq 0.$  Note, however, that in the Bondi model the asymptotic sound speed has a finite value  $a_\infty>0$  while  $v_\infty=0,$  whereas in the present case  $v_\infty>0$  and  $a_\infty\to\infty.$ 

<sup>&</sup>lt;sup>2</sup>The only possible exception being the nearly incompressible, dense interior of a neutron star (Abramowicz et al. 2009; Capela et al. 2013)

Substituting  $\Phi$  from equation (8) into equations (10) and (11) we obtain<sup>3</sup>

$$A_1 = v_{\infty}, \tag{12}$$

$$A_n = 0 \qquad \text{for} \qquad n \ge 2. \tag{13}$$

On the other hand, since we are interested in finding a steady-state solution, we have the additional condition of a constant accretion rate  $\dot{M}$  across any closed surface surrounding the central object. In particular, if we take a sphere of radius r centered at the origin, we have

$$\dot{M} = \int_0^{2\pi} \int_0^{\pi} \rho_{\infty} \left( \vec{v} \cdot \hat{r} \right) r^2 \sin \theta \, d\theta \, d\phi$$

$$= 2\pi r^2 \int_0^{\pi} \rho_{\infty} \left( -\frac{dr}{dt} \right) \sin \theta \, d\theta$$

$$= 4\pi \rho_{\infty} B_0,$$
(14)

which implies that

$$B_0 = \frac{\dot{M}}{4\pi\rho_{\infty}}. (15)$$

Note that at this point we do not have any restriction on the coefficients  $B_n$  for n > 0 since, due to the orthogonality of the Legendre polynomials, it will always be guaranteed that

$$\int_0^{\pi} P_n(\cos \theta) \sin \theta \, d\theta = 0. \tag{16}$$

These higher order multipoles could, in principle, be used to match some given inner boundary condition close to the accretor. In the absence of any such boundary condition (we have assumed a perfect sink as central accretor), we take the lowest order solution given by

$$\Phi = v_{\infty} r \cos \theta + \frac{\dot{M}}{4\pi \rho_{\infty} r},\tag{17}$$

which leads to the velocity field

$$\frac{\mathrm{d}r}{\mathrm{d}t} = v_{\infty} \left( \cos \theta - \frac{s^2}{r^2} \right),\tag{18}$$

$$\frac{\mathrm{d}\theta}{\mathrm{d}t} = -\frac{v_{\infty}}{r}\sin\theta,\tag{19}$$

where we have introduced the stream length scale

$$s = \sqrt{\frac{\dot{M}}{4\pi\rho_{\infty}v_{\infty}}}. (20)$$

An equation for the streamlines can be obtained by combining equations (18) and (19), which results in the differential equation

$$\frac{\mathrm{d}r}{\mathrm{d}\theta} = \frac{s^2 \csc \theta}{r} - r \cot \theta. \tag{21}$$

Equation (21) can be integrated at once to give

$$r = \frac{\sqrt{b^2 - 2s^2(\cos\theta + 1)}}{\sin\theta},\tag{22}$$

where b is an integration constant which we have chosen in such a way that it corresponds to the impact parameter of each streamline, i.e.

$$(r\sin\theta)|_{\theta=\pi} = b. \tag{23}$$

Now that we have an expression for the velocity field and the streamlines of this model; we can proceed to visualize the resulting accretion flow. In Figure 1 we show the streamlines of this model together with isocontours of the magnitude of the velocity field. The red cross in this figure indicates the location of the so-called stagnation point where, according to equations (18) and (19), the velocity field vanishes. From these equations we can see that it is located at r = s,  $\theta = 0$ . On the other hand, from equation (22) we can show that the unique streamline that ends up at the stagnation point is characterized by the critical impact parameter  $b_c = 2s$ . Moreover, this same streamline separates the flow into two regions: all the streamlines with an impact parameter  $b < b_c$  end up accreting onto the central object (constituting thus the accretion basin) while those with  $b > b_c$  escape to infinity.

The pressure can now be recovered from the Bernoulli constant in equation (6) as

$$P = P_{\infty} + \frac{GM \,\rho_{\infty}}{r} + \rho_{\infty} v_{\infty}^2 \frac{s^2}{r^2} \left( \cos \theta - \frac{s^2}{2 \, r^2} \right), \tag{24}$$

where we have used the velocity components given in equations (18) and (19).

From equation (24) we see that P will become negative at sufficiently small radii. In order to prevent this from happening, we can take the accretor to have a finite radius R and require the central object to fully enclose the region where P < 0. Using equation (24), it is easy to see that this condition can be satisfied by taking a sufficiently large value for the asymptotic value of the pressure, namely

$$\frac{P_{\infty}}{\rho_{\infty} v^2} \ge \frac{s^2}{R^2} \left( 1 + \frac{s^2}{2R^2} \right) - \frac{GM}{R v^2}.$$
 (25)

 $<sup>^{3}</sup>$ The coefficient  $A_{0}$  only contributes an additive constant to the velocity potential and, therefore, does not convey any physical information.

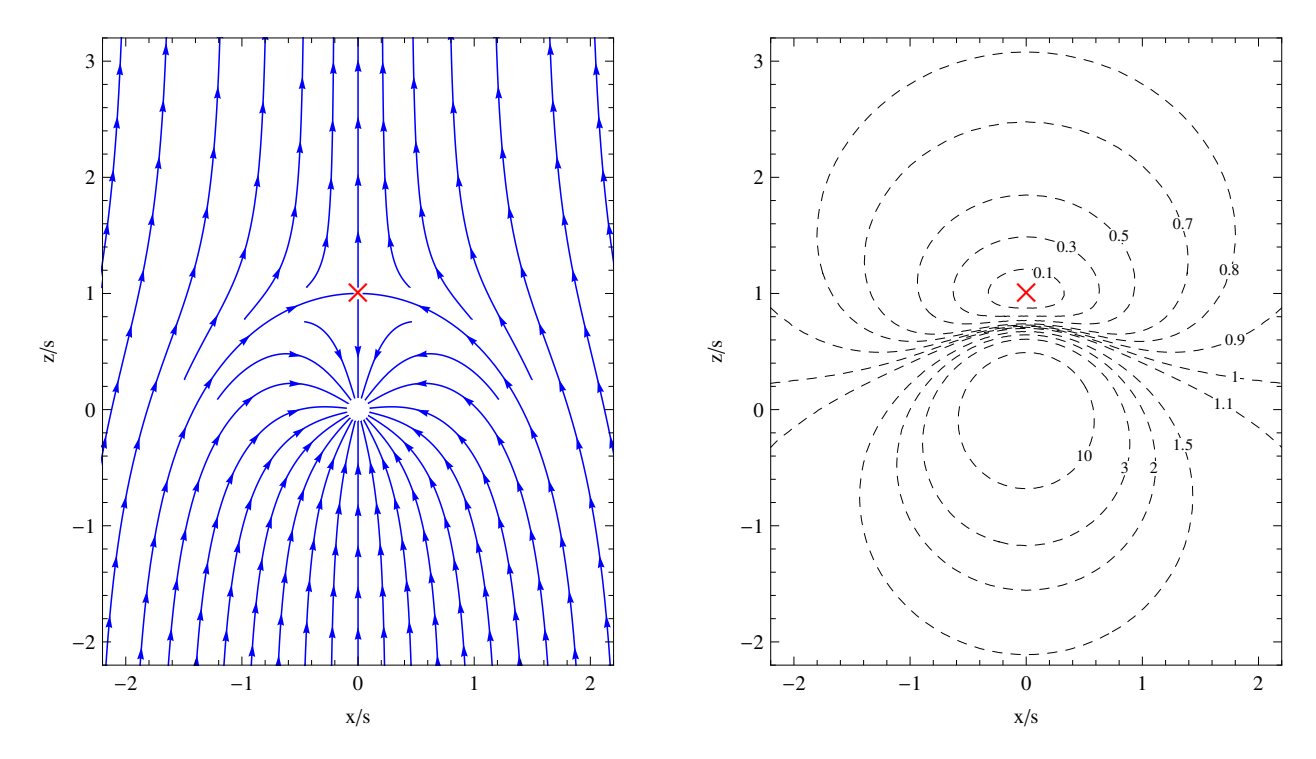


Fig. 1. Wind accretion of an incompressible fluid. The left-hand panel hows the streamlines as described by equation (22). The right-hand panel shows the isocontour levels of the magnitude of the velocity field in equations (18) and (19), the contour labels being expressed in units of  $v_{\infty}$ . The stagnation point is marked with a cross in both panels.

On the other hand, for fixed asymptotic values  $v_{\infty}$ ,  $\rho_{\infty}$ ,  $P_{\infty}$ , and a given central accretor of mass M and radius R, this same condition can be rewritten as an upper limit on the accretion rate:

$$\dot{M} \le 4\pi \,\rho_{\infty} v_{\infty} \,R^2 \left( \sqrt{1 + \frac{2 \,\mathrm{G} M}{R \,v_{\infty}^2}} - 1 \right). \tag{26}$$

Furthermore, in order for the central accretor to behave as a true sink, it is necessary to require that R < s, i.e. for the stagnation point to lie outside the accretor. From equation (20), this condition translates as the following lower limit on the accretion rate

$$\dot{M} > 4\pi \,\rho_{\infty} v_{\infty} \,R^2. \tag{27}$$

Consistency between the two inequalities in equations (25) and (27) imposes the following relationship between the rest of the model's parameters

$$\frac{P_{\infty}}{\rho_{\infty}v_{\infty}^2} + \frac{GM}{Rv_{\infty}^2} > \frac{3}{2}.$$
 (28)

We have thus found that, with this model, we cannot determine a unique accretion rate for a given central object and asymptotic gas properties. In other words,  $\dot{M}$  plays the role of an additional parameter of the model that, at most, should conform

to the range given by equations (26) and (27). This is analogous to the case of Bondi's spherical accretion where, in the absence of any additional inner boundary condition, steady solutions are found for any value of the accretion rate within the range

$$0 \le \dot{M} \le \dot{M}_B \equiv \pi \left(\frac{2}{5 - 3\gamma}\right)^{\frac{5 - 3\gamma}{2(\gamma - 1)}} \frac{(GM)^2}{a_\infty^3} \rho_\infty, \tag{29}$$

where  $\gamma$  is the polytropic index of the equation of state and  $\dot{M}_B$ , the maximum possible accretion rate, corresponds to a transonic solution.

We would like to remark here that the standard result from spherical accretion in equation (29) should be modified when the accretor radius is comparable or larger than the so-called Bondi radius  $R_B = \mathrm{G}M/a_\infty^2$ , in which case the maximum accretion is given by

$$\dot{M} = 4\pi \,\rho_{\infty} a_{\infty} R^2 \left\{ 2 \left( \frac{1 + (\gamma - 1) R_B / R}{\gamma + 1} \right) \right\}^{\frac{\gamma + 1}{2(\gamma - 1)}}.$$
(30)

Note that taking the limit  $v_{\infty} \to 0$  in equation (26) leads to

$$\dot{M} = 4\pi \,\rho_{\infty} \sqrt{2 \,\mathrm{G} M R^3},\tag{31}$$

(37)

which is the same value for the maximum accretion rate that results by taking the limiting case  $\gamma \to \infty$  (that corresponds to  $a \to \infty$ ) in equation (30).

Finally, it is interesting to notice that the equation for the streamlines in equation (22) is independent of both the mass of the central object M and the fluid pressure. In fact, M only affects directly the fluid's pressure via equation (24). Moreover, all of the expressions that we have found remain valid even for M=0 (provided that a massless sink can be conceived in three dimensions). The role played by M>0 is to contribute to a steeper pressure gradient and to confine the region of negative pressure to a smaller volume than the one arising for a massless sink.

## 3. RELATIVISTIC MODEL

The relativistic solution found by Petrich et al. (1988) (PST) describes a wind accreting onto a rotating black hole (Kerr spacetime) under the conditions of stationarity and irrotational flow. Similarly to the Newtonian case, an irrotational flow in general relativity can be described by a velocity potential  $\Phi$  such that<sup>4</sup>

$$h u^{\mu} = g^{\mu\nu} \frac{\partial \Phi}{\partial x^{\nu}}, \tag{32}$$

where  $h=(e+P)/\rho\,c^2$  is the relativistic enthalpy, e the relativistic internal energy density,  $u^\mu=dx^\mu/d\tau$  the four-velocity, and  $g^{\mu\nu}$  the inverse of the spacetime metric. Substituting equation (32) into the continuity equation (in this case  $\nabla_\mu(\rho\,u^\mu)=0$ , where  $\nabla_\mu$  stands for the covariant derivative) leads to

$$g^{\mu\nu}\nabla_{\mu}\left(\frac{\rho}{h}\frac{\partial\Phi}{\partial x^{\nu}}\right) = 0. \tag{33}$$

In general, equation (33) is a non-linear equation in  $\Phi$  except in the special case where  $h \propto \rho$ . Specifically, PST considered a stiff equation of state for which  $P \propto \rho^2$  and  $P = e^{.6}$  With this choice,

the fluid's sound speed is constant and equal to the speed of light c everywhere in the fluid.<sup>7</sup>

In the case of a non-rotating black hole (i.e. Schwarzschild spacetime), PST found the following expression for the velocity potential

$$\Phi = -\Gamma_{\infty} \left[ t c^2 + 2 c r_g \ln \left( 1 - 2 \frac{r_g}{r} \right) - v_{\infty} (r - r_g) \cos \theta \right],$$
(34)

where  $r_g = \mathrm{G}M/\mathrm{c}^2$  is the gravitational radius and  $\Gamma_\infty$  is the Lorentz factor as measured at infinity

$$\Gamma_{\infty} \equiv \left(\frac{\mathrm{d}t}{\mathrm{d}\tau}\right)\Big|_{\infty} = \frac{1}{\sqrt{1 - v_{\infty}^2/\mathrm{c}^2}}.$$
 (35)

Substituting the velocity potential  $\Phi$  into equation (32) leads to the velocity field

$$\rho \frac{\mathrm{d}t}{\mathrm{d}\tau} = \Gamma_{\infty} \rho_{\infty} \left( 1 - 2 \frac{r_g}{r} \right)^{-1} , \qquad (36)$$

$$\rho \frac{\mathrm{d}r}{\mathrm{d}\tau} = \Gamma_{\infty} \rho_{\infty} \left[ v_{\infty} \left( 1 - 2 \frac{r_g}{r} \right) \cos \theta - 4 c \frac{r_g^2}{r^2} \right] ,$$

$$\rho \frac{\mathrm{d}\theta}{\mathrm{d}\tau} = -\Gamma_{\infty} \, \rho_{\infty} \frac{v_{\infty}}{r^2} (r - r_g) \sin \theta. \tag{38}$$

The special restrictions that arise in general relativity from demanding a regular solution across the black hole's event horizon (located at  $2\,r_g$  for a Schwarzschild spacetime) imply that the PST model is characterized by the unique accretion rate

$$\dot{M} = 16\pi \frac{(GM)^2}{c^3} \rho_{\infty} \Gamma_{\infty}.$$
 (39)

This is an important difference with respect to the Newtonian solution discussed in the previous section where the accretion rate was a free parameter [at most restricted by the inequalities in equations (26) and (27)].

Let us now define the constant

$$\sigma = \sqrt{\frac{\dot{M}}{4\pi\rho_{\infty}v_{\infty}\Gamma_{\infty}}} = \frac{s}{\sqrt{\Gamma_{\infty}}},\tag{40}$$

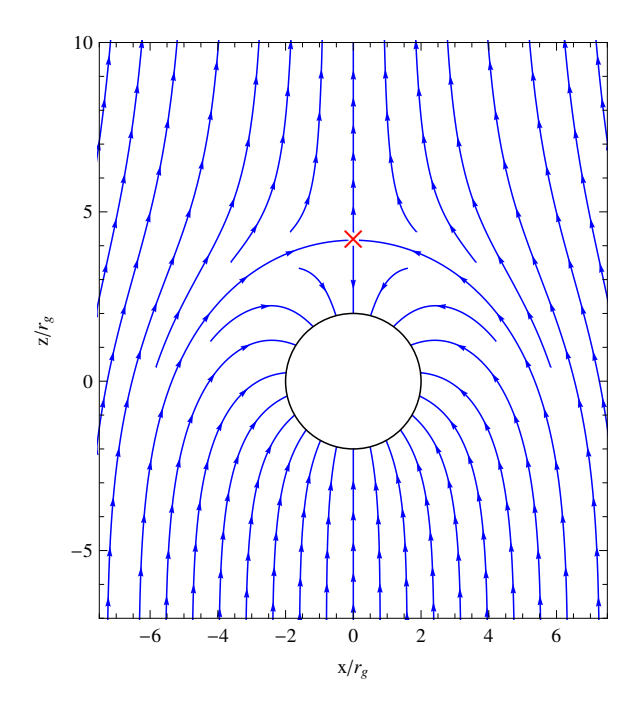
as a natural extension of the stream length scale s introduced in equation (20). Using this definition together with equation (36), we can rewrite the velocity components in equations (37) and (38) in terms

 $<sup>^4</sup>$  Greek indices run over spacetime components, e.g.  $x^\mu=$  (c  $t,\,r,\,\theta,\,\phi).$  We adopt Einstein's summation convention over repeated indices.

<sup>&</sup>lt;sup>5</sup>In the PST paper the authors use the symbol  $\rho$  to denote the relativistic internal energy density and work with the baryon number density n. For an average baryonic rest mass m, n is related to the rest mass density by  $\rho = m n$ .

<sup>&</sup>lt;sup>6</sup>The relativistic energy density is defined as  $e = \rho(u+c^2)$ , where u is the non-relativistic internal energy (per unit mass). For a polytropic equation of state  $P = K \rho^2$  one has  $u = K \rho$ . Thus, the equations  $P \propto \rho^2$  and P = e are incompatible unless the rest-mass energy is negligible compared to the internal energy, i.e.  $u \gg c^2$ . These two equations will also be compatible for the case of a massless scalar field, in which case the number density n plays the role of a comoving marker.

<sup>&</sup>lt;sup>7</sup>The relativistic expression for the sound speed is  $a = c\sqrt{\partial P/\partial \rho|_s}$  as opposed to  $a = \sqrt{\partial P/\partial \rho|_s}$  in non-relativistic physics.



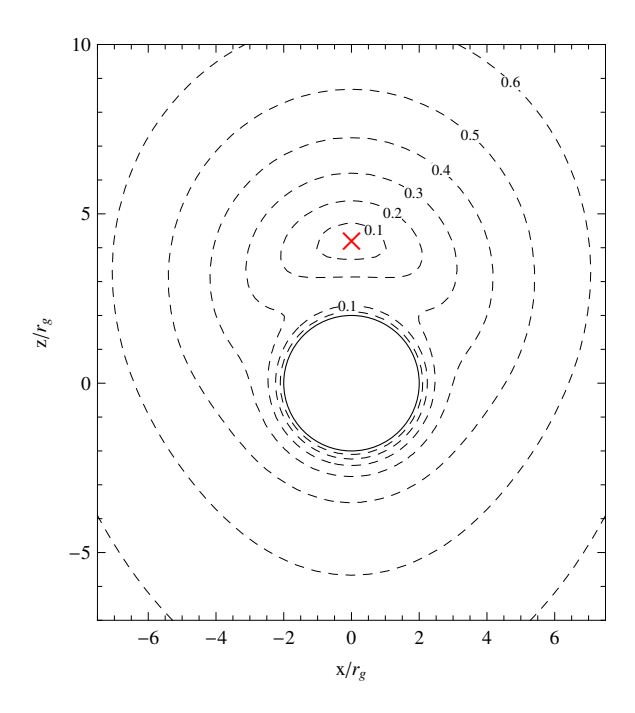


Fig. 2. Wind accretion of the PST model for a Schwarzschild black hole. In this case we have taken  $\sigma=3\,r_g$  (which corresponds to  $v_\infty\simeq 0.44\,\mathrm{c}$ ). The left-hand panel shows the streamlines as described by equation (45). The right-hand panel shows the isocontour levels of the magnitude of the velocity field in equations (41) and (42), the contour labels being expressed in units of  $v_\infty$ . The stagnation point (located at  $\theta=0$ ,  $r=r_g+(r_g^2+\sigma^2)^{1/2}\simeq 4.2\,r_g$ ) is marked with a cross in both panels. The black circle shows the black hole's event horizon located at the Schwarzschild radius  $2\,r_g$ .

of the coordinate time t as

$$\frac{\mathrm{d}r}{\mathrm{d}t} = v_{\infty} \left( 1 - 2 \frac{r_g}{r} \right) \left[ \left( 1 - 2 \frac{r_g}{r} \right) \cos \theta - \frac{\sigma^2}{r^2} \right], \tag{41}$$

$$\frac{\mathrm{d}\theta}{\mathrm{d}t} = -\frac{v_{\infty}}{r} \left( 1 - 2\frac{r_g}{r} \right) \left( 1 - \frac{r_g}{r} \right) \sin \theta. \tag{42}$$

Just as in the Newtonian case, an equation for the streamlines can be obtained by first combining equations (41) and (42) as (Karas & Mucha 1993)

$$\frac{\mathrm{d}r}{\mathrm{d}\theta} = \frac{\sigma^2 \csc \theta}{r - r_g} - r \left(\frac{r - 2r_g}{r - r_g}\right) \cot \theta, \tag{43}$$

and then integrating this differential equation to obtain the following expression

$$r = r_g + \sqrt{\frac{b^2 - 2\sigma^2(\cos\theta + 1)}{\sin^2\theta} + r_g^2},$$
 (44)

where, as before, the integration constant b corresponds to the impact parameter characterizing each individual streamline.

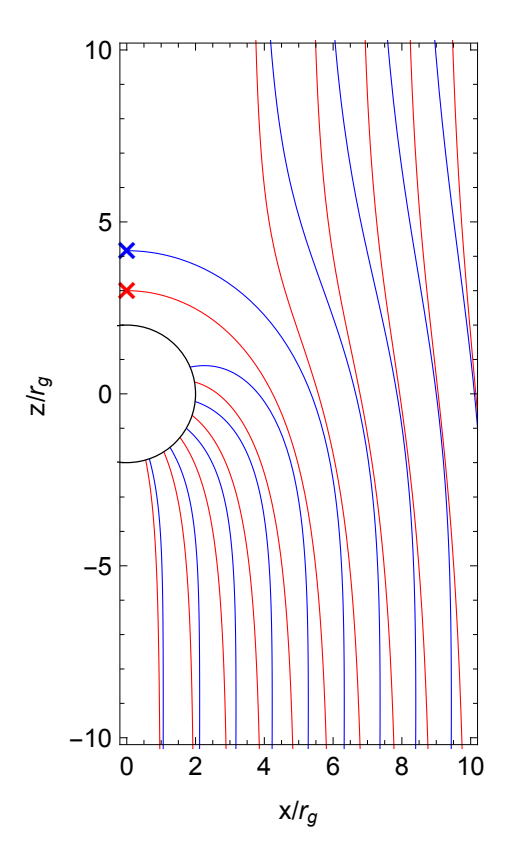
From the velocity components in equations (41) and (42) we can see that the stagnation point in this case is located at  $r = r_g + (r_g^2 + \sigma^2)^{1/2}$ ,  $\theta = 0$ . Completely analogously to the Newtonian case, from equation (44) we can show that the critical impact parameter  $b_c = 2 \sigma$  corresponds to the unique

streamline ending up at the stagnation point. By combining equations (39) and (40) we obtain the following relationship between the stream length scale  $\sigma$  and the wind speed at infinity

$$\frac{v_{\infty}}{c} = 4 \frac{r_g^2}{\sigma^2},\tag{45}$$

from which we can see that even in the limit  $v_{\infty} \to c$ , the stagnation point reaches a minimum radius of  $r \simeq 3.2\,r_g$ , i.e. it is always located outside the event horizon.

In Figure 2 we show the streamlines and isocontour levels of the velocity field of the PST model for the particular case  $\sigma=3\,r_g$  which, from equation (45), corresponds to a wind speed at infinity of  $v_\infty\simeq 0.44\,\mathrm{c}$ . From this figure [and also from equations (41) and (42)] we can see that, in addition to the stagnation point, the velocity field also vanishes at the event horizon  $r=2\,r_g$ . This is only a coordinate effect related to the fact that the light cones close onto themselves when described in terms of the coordinate time t, which implies that t is not well suited for describing physical processes close to the event horizon. Indeed, from equations (36)–(38), we can see that the velocity components  $\mathrm{d}r/\mathrm{d}\tau$  and  $\mathrm{d}\theta/\mathrm{d}\tau$  do not show this behavior.



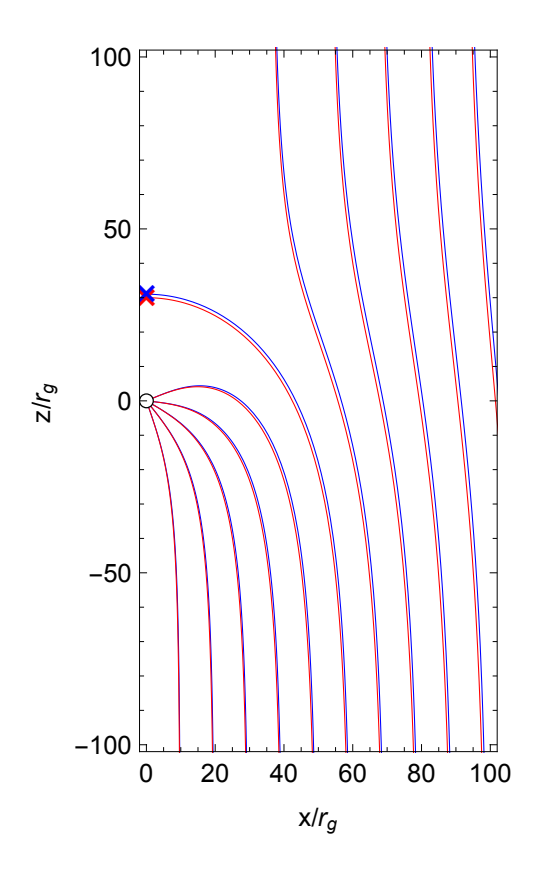


Fig. 3. Comparison between the streamlines of the relativistic PST model (blue lines) and the Newtonian model discussed in § 2 (red lines). In the left-hand panel we have taken  $s=\sigma=3\,r_g$  ( $v_\infty\simeq0.4\,\mathrm{c}$ ) while, for the right-hand one we have  $s=\sigma=30\,r_g$  ( $v_\infty\simeq0.004\,\mathrm{c}$ ). Pairs of streamlines originate from the exact same point at infinity ( $\theta=\pi$ ) with uniformly distributed impact parameters  $b=r_g,\,2\,r_g,\,3\,r_g,\ldots$  (left panel) and  $b=10\,r_g,\,20\,r_g,\,30\,r_g,\ldots$  (right panel). In both panels, the black circle shows the black hole's event horizon located at the Schwarzschild radius  $2\,r_g$ . The color figure can be viewed online.

Contrary to the Newtonian model where the resulting flow was described by only one characteristic length scale, namely the stream length scale s, the relativistic model is characterized by two length scales: the stream length scale  $\sigma$  and the gravitational radius  $r_q$ .

Also in contrast to the Newtonian solution, the rest mass density  $\rho$  in the PST model is not constant. An expression for  $\rho$  can be found by imposing the normalization condition of the four-velocity  $(g_{\mu\nu}u^{\mu}u^{\nu}=-c^2)$  in equations (36)–(38), which results in

$$\rho = \Gamma_{\infty} \rho_{\infty} \left[ \left( 1 + 2 \frac{r_g}{r} \right) \left( 1 + 4 \frac{r_g^2}{r^2} \right) + 8 \frac{v_{\infty}}{c} \frac{r_g^2}{r^2} \cos \theta - \frac{v_{\infty}^2}{c^2} \left( 1 - 2 \frac{r_g}{r} + \frac{r_g^2}{r^2} \sin^2 \theta \right) \right]^{1/2}.$$
(46)

Let us now consider the non-relativistic limit, that is, the regime in which  $v_{\infty}/c \ll 1$  and  $r_g/r \ll 1$ . Within this limit, we have that  $\Gamma_{\infty} \to 1$  and  $\sigma \to s$ . It then follows that the velocity components in equations (41) and (42) reduce to the ones corresponding to the Newtonian model in equations (18) and (19). On the other hand, from the expression for the rest mass density in equation (46), it follows that  $\rho \to \rho_{\infty} = \text{const.}$  In other words, within the non-relativistic limit we recover the incompressible flow approximation on which we based our Newtonian solution.

Finally, in order to facilitate the comparison between the Newtonian and the PST models, in Figure 3 we show the corresponding streamlines side by side for two cases:  $s = \sigma = 3 \, r_g$  and  $s = \sigma = 30 \, r_g$ . From equation (45) it is simple to see that  $\sigma \gg r_g$  implies  $v_{\infty} \ll c$ . Therefore, as the ratio  $\sigma/r_g$  grows,

the non-relativistic limit should be recovered, just as we can confirm by comparing the left and right panels of this figure.

# 4. SUMMARY

In this paper, we have presented a simple analytic model of wind accretion for an incompressible fluid falling onto a massive gravitating object. We have shown that this model constitutes a probe into the highly subsonic regime with  $\mathcal{M} \simeq 0$ . Moreover, this solution corresponds to the Newtonian limit of the relativistic model of wind accretion onto a black hole found by Petrich et al. (1988) (PST). The fluid in the PST model obeys a stiff equation of state P=e for which the sound speed is constant everywhere and equal to the speed of light. In hindsight, it is not surprising that the Newtonian limit of such a fluid corresponds precisely to an incompressible fluid for which the sound speed is, formally, equal to infinity.

The incompressible fluid approximation effectively decouples the flow dynamics from the central object's gravitational field. This is reflected in the fact that the expression for the streamlines given in equation (22) is independent of the accretor mass M. Only the fluid's pressure is directly influenced by M, as expressed in equation (24). We have found that as M increases, the pressure gradient becomes steeper so as to oppose the enhanced gravitational attraction, and, at the same time, the negative pressure region becomes confined to a smaller volume.

The Newtonian model features only one characteristic length scale: the stream length scale  $s=(\dot{M}/4\pi\rho\,v_\infty)^{1/2}$ . In addition to this the PST model is also characterized by the gravitational radius  $r_g={\rm G}M/{\rm c}^2$ . The existence of these two characteristic length scales leads to a richer variety of flow morphologies than that of the Newtonian model (see Figure 3). The Newtonian model is recovered in the limit  $s\gg r_g$  which naturally coincides with the non-relativistic limit  $v_\infty\ll c$ .

Another difference between the Newtonian and relativistic models is that, in the former, the accretion rate  $\dot{M}$  is an external parameter of the model (at most restricted by the inequalities in equations (26) and (27)) while, in the latter, it has to have the fixed value  $\dot{M}=16\pi({\rm G}M)^2\rho_{\infty}\Gamma_{\infty}/{\rm c}^3$  in order to guarantee a regular solution across the black hole's event horizon.

The Newtonian model presented in this article can be used as an illustrative example in a gas dynamics course. Moreover, it should be useful as a benchmark for testing Newtonian hydrodynamics codes.

I gratefully acknowledge John Miller, Sergio Mendoza and Olivier Sarbach for helpful comments and suggestions. This work was supported by the CONACYT grants 290941 and 291113.

#### REFERENCES

Abramowicz, M. A., Becker, J. K., Biermann, P. L., et al. ApJ, 705, 659

Banyuls, F., Font, J. A., Ibáñez, J. M., Martí, J. M., & Miralles, J. A. 1997, ApJ, 476, 221

Bondi, H. 1952, MNRAS, 112, 195

Bondi, H. & Hoyle, F. 1944, MNRAS, 104, 273

Capela, F., Pshirkov, M., & Tinyakov, P. 2013, PhRvD, 87, 123524

Cruz-Osorio, A., Lora-Clavijo, F. D., & Guzmán, F. S. 2012, MNRAS, 426, 732

Duez, M. D., Foucart, F., Kidder, L. E., et al. 2008, PhRvD, 78, 104015

Edgar, R. 2004, NewAR, 48, 843

Foglizzo, T., Galletti, P., & Ruffert, M. 2005, A&A, 435, 397

Font, J. A. & Ibáñez, J. M. 1998, ApJ, 494, 297

Hoyle, F. & Lyttleton, A. 1939, Mathematical Proceedings of the Cambridge Philosophical Society, 35, 405Hunt, R. 1971, MNRAS, 154, 141

Jackson, J. D. 1998, Classical electrodynamics

Karas, V. & Mucha, R. 1993, AmJPh, 61, 825

Matsuda, T., Sekino, N., Sawada, K., etters Shima, E., Livio, M., Anzer, U., & Boerner, G. 1991, A&A, 248, 301

Michel, F. C. 1972, Ap&SS, 15, 153

Moeckel, N. & Throop, H. B. 2009, ApJ, 707, 268

Petrich, L. I., Shapiro, S. L., Stark, R. F., & Teukolsky, S. A. 1989, ApJ, 336, 313

Petrich, L. I., Shapiro, S. L., & Teukolsky, S. A. 1988, PhRvL, 60, 1781

Ruffert, M. & Arnett, D. 1994, ApJ, 427, 351

Shima, E., Matsuda, T., Takeda, H., & Sawada, K. 1985, MNRAS, 217, 367

Zanotti, O., Roedig, C., Rezzolla, L., & Del Zanna, L. 2011, MNRAS, 417, 2899

Emilio Tejeda: Instituto de Astronomía, Universidad Nacional Autónoma de México, AP 70-263, Ciudad de México, 04510, México (etejeda@astro.unam.mx).